Polymer Adsorption on Rough Surfaces. 2. Good Solvent Conditions

Hong Ji

Department of Physics, University of California, Santa Barbara, California 93106

Daniel Hone*

Institute for Theoretical Physics, University of California, Santa Barbara, California 93106.
Received November 3, 1987

ABSTRACT: We present a mean-field study of adsorption on a rough surface of a polymer in a good solvent. We first investigate the influence of surface curvature by considering the adsorption on a sphere. Both a perturbation expansion and numerical calculation show that the surface tension tends to be lowered when the surface is curved toward the polymer solution, whereas it increases when the surface is curved away from the solution. For the polymer solution confined to the interior of a sphere, it is found that there exists a critical sphere radius at which the surface tension is minimized. Adsorption on a sinusoidal grating is then studied by numerical calculation. Detailed results are obtained for the concentration profile and surface excess in various limits.

I. Introduction

The physics of polymer adsorption on surfaces has attracted much interest[1-9] in the past 20 years, at least in part due to its practical application to processes like colloidal particle stabilization, polymer coating, wetting, and adhesion. However, most work has focused on the problem of adsorption on a flat surface. In the first paper of this series[10] we studied the rough surface adsorption for a single ideal chain (no excluded volume interaction between monomers). Here we present a mean-field approach to adsorption on a rough surface from a semidilute polymer solution in a good solvent.

In section II we discuss the formulation of mean-field theory to be adopted here. We use this approach in section III to study the effect of surface curvature on polymer adsorption by considering the adsorption on either the exterior or the interior surface of a sphere. We conclude that if the surface is curved away from the solution, the surface tension and the monomer density on the surface will both be lowered, whereas if the surface is curved toward the solution, they will both increase relative to their values for adsorption on a flat surface. The surface excess per unit area has its maximum value when the size of the sphere is of the order of the adsorption thickness D associated with the strength of the surface attraction.

In section IV, we use a sinusoidal grating to represent the important features of a rough surface, as we did in our paper[10] on the ideal chain. By numerically solving the nonlinear differential equation for the monomer concentration, we obtain the density distribution of monomers in various limits of the surface shape, as described by the surface amplitude and wavelength. If the amplitude is small or the wavelength is long compared with the correlation length of the polymer solution, the distribution differs from that on the flat surface only by small perturbational corrections. When the amplitude is high and the wavelength short, it is found that the polymer density becomes very high in the valleys between the peaks of the surface. We argue that this is due to the increased surface area available for adsorption of the monomers. A study of the surface excess per unit surface area shows that it slowly increases with the surface roughness. These results are discussed further in section V.

II. Formulation

Within the Cahn[11] approach to the interfacial properties of a dilute solution the surface energy is written as

$$U - U_0 = -\gamma_1 \int \mathrm{d}S\, \phi + \int \mathrm{d}V\, [G(\phi) + L(\phi)(\nabla\phi)^2] \tag{II.1}$$

Here U_0 is the surface energy of the pure solvent, ϕ is the solute volume fraction, γ_1 is a local solute–interface interaction energy per unit area (for adsorbing walls $\gamma_1 > 0$, and $\gamma_1 < 0$ for repulsive walls), $G(\phi)$ is an interaction term, and $L(\phi)$ is a function that describes the stiffness of the solution with respect to slow spatial fluctuations of the concentration. The first integral represents the local contact energy between the wall and the solute; the second integral is associated with the deformation of the concentration profile in the vicinity of the surface.

In mean-field theory, the Flory–Huggins free energy density for a uniform semidilute polymer solution is[12]

$$F(\phi) = (T/a^3)\left[\frac{\phi}{N}\ln\phi + \frac{1}{2}v\phi^2 + \frac{1}{6}w\phi^3 + \ldots\right] \tag{II.2}$$

where a is a monomer dimension, N is the molecular weight, and T is the temperature. The first term represents the translational entropy of a polymer chain; v and w are, respectively, the second and third virial coefficients (dimensionless) associated with monomer–monomer interactions. For a semidilute polymer solution ($\phi \ll 1$) the first term is usually neglected, since N is large. Further, in a good solvent $v \sim w$, and the interaction is dominated by the effective two-body repulsions between monomers. Thus we can replace $G(\phi)$ by the second virial term $(T/a^3)(v\phi^2/2)$. In the case of a binary mixture of small molecules, the stiffness function $L(\phi)$ is independent of ϕ, whereas for a polymer solution it is strongly ϕ-dependent.[13] In mean-field theory

$$L(\phi) = (T/a^3)(a^2/24\phi) \tag{II.3}$$

which leads in bulk solution to a structure factor (or density correlation function) of the Ornstein–Zernike form with the Edwards[14] correlation length $\xi_E \sim \phi^{-1/2}$.

For a semidilute polymer solution in a good solvent, the mean-field free energy due to the surface can then be written as

$$U - U_0 = -\gamma_1 \int \mathrm{d}S\, \phi + (T/a^3)\int \mathrm{d}V \left[\frac{1}{2}v\phi^2 + \frac{a^2}{24\phi}(\nabla\phi)^2\right] \tag{II.4}$$

0024-9297/88/2221-2600$01.50/0

It is usually convenient to write the free energy in terms of a mean-field order parameter ψ defined as $\phi = \psi^2$. Then eq II.4 becomes

$$U - U_0 = -\gamma_1 \int dS\, \psi^2 + (T/a^3) \int dV \left[\frac{1}{2} v\psi^4 + \frac{a^2}{6} (\nabla\psi)^2 \right] \quad \text{(II.5)}$$

with the constraint that the total number of monomers be conserved:

$$\int dV\, \psi^2 = \text{constant} \quad \text{(II.6)}$$

The mean field concentration profile $\phi(\vec{r})$ is given by minimizing the free energy with variations in the profile and the surface distribution under the constraint given in (II.6). If the profile in the bulk is fixed and ψ is varied on the surface, minimization of the free energy then gives the boundary condition satisfied by ψ as

$$\left[\frac{\partial\psi}{\partial n} + \kappa\psi \right]_s = 0 \quad \text{(II.7)}$$

where n indicates the normal to the surface, and κ is

$$\kappa = 6\gamma_1 a/T \quad \text{(II.8)}$$

The length κ^{-1} characterizes the strength of surface attraction to monomers. For $\kappa^{-1} > \xi_E$ the monomer–monomer interaction dominates the attraction to the wall, and this leads to weak adsorption, whereas $\kappa^{-1} < \xi_E$ corresponds to strong adsorption.

If we fix ψ on the surface, the Euler–Lagrange equation derived from (II.5) and (II.6) is then

$$\nabla^2\psi + \epsilon\psi - \frac{6v}{a^2}\psi^3 = 0 \quad \text{(II.9)}$$

where ϵ is the Lagrange multiplier. Far from the surface the bulk concentration is a constant, ϕ_b, and $\nabla^2\psi \to 0$. Then ϵ is determined from eq II.9:

$$\epsilon = 6v\phi_b/a^2 \quad \text{(II.10)}$$

and eq II.7 and II.9 can be rewritten as

$$\tilde{\nabla}^2\theta = 2\theta(\theta^2 - 1) \quad \text{(II.11)}$$

$$\left[\frac{\partial\theta}{\partial\tilde{n}} + \tilde{\kappa}\theta \right]_s = 0 \quad \text{(II.12)}$$

where θ is the mean-field order parameter normalized to the bulk concentration: $\theta^2 = \phi/\phi_b$. These are the two equations that determine the distribution of monomers near the surface. We note that they have been written in dimensionless form, with lengths measured in units of the Edwards correlation length, $\xi_E = a/(3v\phi_b)^{1/2}$ (e.g., $\tilde{\kappa} = \kappa\xi_E$), and the Laplacian $\tilde{\nabla}^2$ operates on the dimensionless coordinate $\tilde{x} \equiv x/\xi_E$. Thus the shape of the concentration profile depends only on the *relative* strength of the monomer–monomer interaction and the attraction to the surface.

In terms of this order parameter, the adsorption energy can be conveniently written as

$$U - U_0 = \frac{T\phi_b\xi_E}{6a}\left[-\tilde{\kappa} \int d\tilde{S}\, \theta^2 + \int d\tilde{V}\, [(\theta^2 - 1)^2 + (\tilde{\nabla}\theta)^2] \right] \quad \text{(II.13)}$$

The integrals inside the bracket are over dimensionless lengths x/ξ_E. Notice that both terms inside the bracket are dimensionless.

If the polymer solution is confined to the interior of a closed surface, ϕ_b and ξ_E no longer represent the bulk concentration and correlation length, since "bulk" conditions are never truly obtained within the finite volume. However, they are still the characteristic concentration and correlation length in the problem; they are set by the total number of monomers within the enclosed volume.

III. Adsorption on a Sphere

A. Perturbation Calculations. We begin by recalling the solution for polymer adsorption on a planar surface.[3] The problem is one dimensional, with the concentration profile given by equations II.11 and II.12:

$$\theta = \coth(\tilde{z} + \tilde{z}_0) \quad \text{(III.1)}$$

We recall that the lengths in the problem are measured in units of the Edwards correlation length ξ_E, so that $\tilde{z} = z/\xi_E$ and $\tilde{z}_0 = z_0/\xi_E$. The constant of integration z_0 is determined by the boundary condition (II.12).

We will consider only the weak adsorption limit in order to keep the mathematics tractable. In this limit, $\tilde{\kappa} \ll 1$, the attraction of the wall is much weaker than the monomer–monomer interaction, and the concentration profile is only slightly perturbed by the wall. To first order in $\tilde{\kappa}$ we have

$$\theta \approx 1 + \tilde{\kappa}e^{-2\tilde{z}}/2 \quad \text{(III.2)}$$

The surface energy per unit area, which is the change in surface tension due to the adsorption, is then given by eq II.13:

$$\gamma - \gamma_0 \approx \left(\frac{T\phi_b}{6a\xi_E} \right)\left(-\tilde{\kappa} - \frac{\tilde{\kappa}^2}{2} \right) \quad \text{(III.3)}$$

where we have kept terms only up to order $\tilde{\kappa}^2$.

Suppose now that the surface is slightly bent into a sphere of large radius. There are two ways to bend the surface, either toward or away from the polymer solution (the solution then being confined either to the interior or to the exterior of the sphere, respectively). In both cases, at sufficiently large spherical radius ($\gg\xi_E$) the corrections to the normalized order parameter θ from unity are small (since we still assume $\tilde{\kappa} \ll 1$):

$$\theta = 1 + \delta \qquad (\delta \ll 1) \quad \text{(III.4)}$$

Then we can to a good approximation linearize eq II.11 and II.12 with respect to δ and solve these equations in spherical coordinates to get the perturbational solutions.

If we use suffixes *out* and *in* to denote the two cases where we have polymer solution outside and within the sphere, respectively, we can write the perturbational solutions as

$$\theta_{out}(\tilde{r}) \approx 1 + \frac{\tilde{\kappa}\tilde{b}}{2\tilde{b} + 1}\left(\frac{\tilde{b}}{\tilde{r}} \right) e^{-2(\tilde{r} - \tilde{b})} \qquad (\tilde{b} < \tilde{r} < \infty) \quad \text{(III.5)}$$

$$\theta_{in}(\tilde{r}) \approx 1 + \tilde{\kappa}\tilde{b}\left(\frac{\tilde{b}}{\tilde{r}} \right) \frac{\sinh 2\tilde{r}}{2\tilde{b}\cosh 2\tilde{b} - \sinh 2\tilde{b}} \qquad (0 < \tilde{r} < \tilde{b}) \quad \text{(III.6)}$$

where we have kept terms only to first order in $\tilde{\kappa}$. Here b is the radius of the sphere, and again all lengths are measured in units of the Edwards correlation length ξ_E: $\tilde{r} = r/\xi_E$ and $\tilde{b} = b/\xi_E \gg 1$.

For the monomer concentration on the surface we have

$$\theta_{out}(\tilde{b}) \approx 1 + \frac{\tilde{\kappa}}{2}\left(1 - \frac{1}{2\tilde{b}} \right) \quad \text{(III.7)}$$

$$\theta_{in}(\tilde{b}) \approx 1 + \frac{\tilde{\kappa}}{2}\left(1 + \frac{1}{2\tilde{b}} \right) \quad \text{(III.8)}$$

where we have kept only first-order corrections in $1/\tilde{b}$. Comparing with the flat surface case, where the monomer concentration on the surface is $\theta_0 \approx 1 + \tilde{\kappa}/2$, we see that $\theta_{out}(\tilde{b}) < \theta_0$ and $\theta_{in}(\tilde{b}) > \theta_0$.

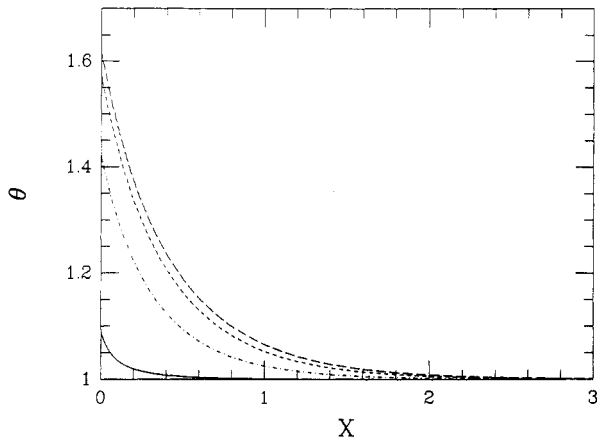

Figure 1. Concentration profiles for polymer adsorption on spheres: $\tilde{\kappa} = 1$; $\tilde{b} = 0.1$ (solid line), 1 (dot dashed), 5 (short dashes), and 100 (long dashes). X represents the distance from the surface in units of ξ_E: $X = \tilde{r} - \tilde{b}$.

Turning next to the change in surface tension due to the surface curvature, we use the concentration profiles of eq III.5 and III.6 in eq II.13 to find

$$\gamma_{out} - \gamma_0 \approx \frac{T\phi_b}{6a\xi_E}\left(-\tilde{\kappa} - \frac{\tilde{\kappa}^2}{2} + \frac{\tilde{\kappa}^2}{4\tilde{b}}\right) \quad \text{(III.9)}$$

$$\gamma_{in} - \gamma_0 \approx \frac{T\phi_b}{6a\xi_E}\left(-\tilde{\kappa} - \frac{\tilde{\kappa}^2}{2} - \frac{\tilde{\kappa}^2}{4\tilde{b}}\right) \quad \text{(III.10)}$$

Comparing with the flat-surface case, we see that when the surface curves sufficiently gently that this lowest order perturbation approximation is valid, bending of the surface toward the polymer solution will cause the surface tension to decrease, whereas bending away from the solution causes the surface tension to increase.

B. Numerical Calculations. To understand the effect of more rapid (higher curvature) surface variations on polymer adsorption, we have made numerical calculations for spherical surfaces of relatively small radius. As in the perturbation calculation above, we treat separately the cases of polymer solution outside and inside the sphere.

1. Polymer Solution outside a Sphere. In spherical coordinates, with only radial dependences (by symmetry) the basic equations (II.11 and II.12) become

$$\frac{d^2\theta}{d\tilde{r}^2} + \frac{2}{\tilde{r}}\frac{d\theta}{d\tilde{r}} = 2\theta(\theta^2 - 1) \quad \text{(III.11)}$$

$$\left[\frac{d\theta}{d\tilde{r}} + \tilde{\kappa}\theta\right]_{\tilde{r}=\tilde{b}} = 0 \quad \text{(III.12)}$$

The boundary condition at $\tilde{r} \to \infty$ is that $\theta \to 1$.

From eq II.13, the surface tension in this problem can be written as

$$\gamma_{out} - \gamma_0 = \frac{T\phi_b}{6a\xi_E}\left[-\tilde{\kappa}\theta^2(\tilde{b}) + \int_{\tilde{b}}^{\infty}[(\theta^2 - 1)^2 + (\tilde{\nabla}\theta)^2]\left(\frac{\tilde{r}}{\tilde{b}}\right)^2 d\tilde{r}\right] \quad \text{(III.13)}$$

Note that the quantities within the brackets are written in dimensionless form. The surface excess in this case can be written as

$$\Gamma a^3 = \xi_E\phi_b\int_{\tilde{b}}^{\infty}(\theta^2 - 1)\left(\frac{\tilde{r}}{\tilde{b}}\right)^2 d\tilde{r} \quad \text{(III.14)}$$

Figure 1 shows the concentration profiles as calculated from eq III.11 and III.12 for several values of the radius of the sphere. The monomer concentration on the surface decreases with decreasing radius of the sphere. Figure 2

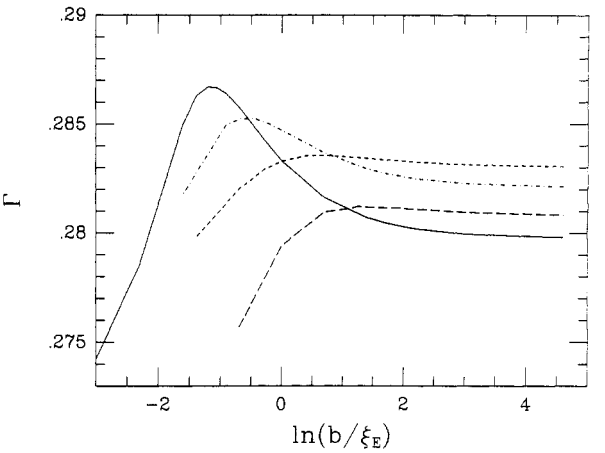

Figure 2. Surface excess for polymer adsorption on spheres: $\tilde{\kappa} = 5$ (solid line), 3 (dot dashed), 1 (short dashes), and 0.5 (long dashes). The scale of the ordinate, Γ, is arbitrary and *different for each curve*; the actual peak surface excess varies by more than an order of magnitude over the range of $\tilde{\kappa}$ shown.

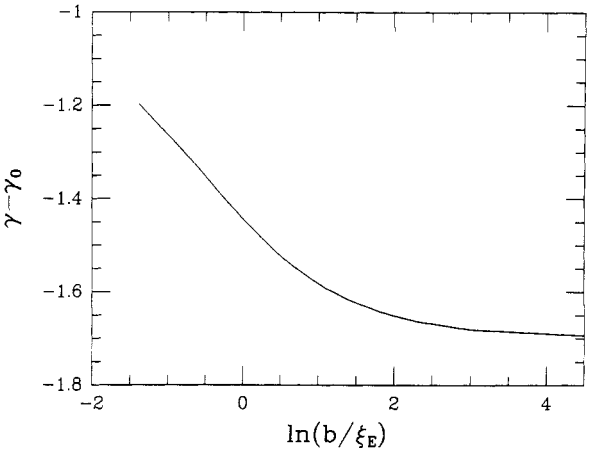

Figure 3. Surface tension $\gamma - \gamma_0$, in units of $T\phi_b\xi_E/(6a)$, as a function of sphere radius $\tilde{b}$.

is a plot of surface excess as a function of the radius for four different values of κ. The radius where the surface excess has its maximum is approximately $r^* \approx 1.35\kappa^{-1}$.

Figure 3 is a plot of the dependence of surface tension on the radius of the sphere. We see that as the radius of the sphere decreases, the surface tension increases monotonically from its flat surface value. We shall discuss these results in section V.

2. Polymer Solution inside a Sphere. We consider next the case where the polymer solution is confined to the interior of a sphere, with adsorption on the inner surface thereof. Since for this geometry it is no longer appropriate to consider the polymer solution to be in contact with a reservoir at given concentration ϕ_b, we will fix the total number of monomers inside the sphere and study the concentration profile and surface tension as functions of the radius of the sphere.

The equations that determine the concentration profile are

$$\frac{d^2\theta}{d\tilde{r}^2} + \frac{2}{\tilde{r}}\frac{d\theta}{d\tilde{r}} = 2\theta(\theta^2 - 1) \quad \text{(III.15)}$$

$$\left[\frac{d\theta}{d\tilde{r}} - \tilde{\kappa}\theta\right]_{\tilde{r}=\tilde{b}} = 0 \quad \text{(III.16)}$$

and the constraint on the total number of monomers is

$$Na^3 = \phi_b\xi_E{}^3\int_0^{\tilde{b}} 4\pi\tilde{r}^2\theta^2\, d\tilde{r} \quad \text{(III.17)}$$

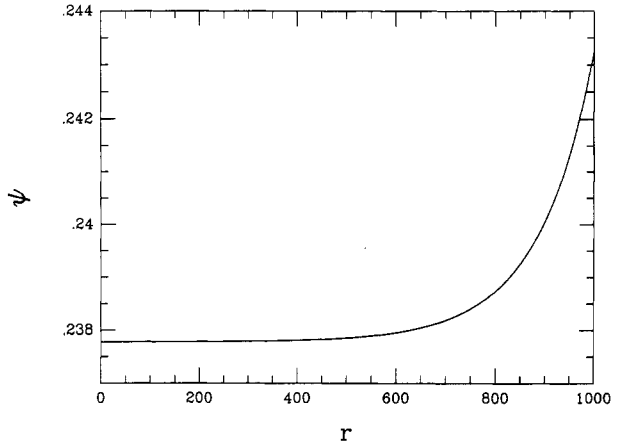

Figure 4. Concentration profile for polymer adsorption in the interior of a sphere. Here $b = 1000$ Å, $\kappa = 10^{-4}$ Å^{-1}, $3v/a^2 = 10^{-4}$ Å^{-2}, and the total number of monomers is $N = 10^9$.

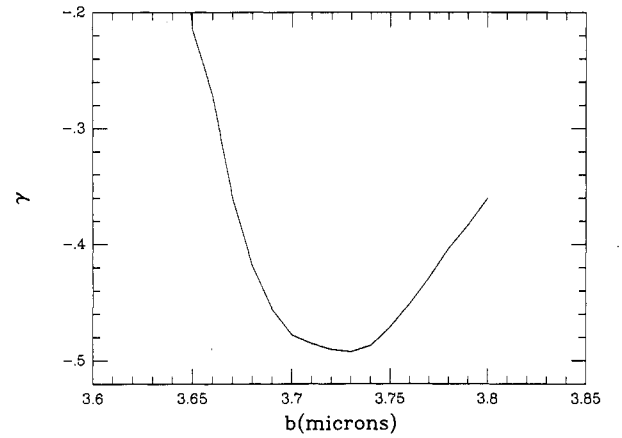

Figure 5. Surface tension $\gamma - \gamma_0$ (in arbitrary units), as a function of sphere radius b, with the polymer solution confined to the interior of the sphere. Here $\kappa = 10^{-4}$ Å^{-1}, total number of monomers $N = 10^9$, and $3v/a^2 = 0.1$ Å^{-2}.

The condition at $\tilde{r} = 0$ is, by symmetry, $d\theta/d\tilde{r} = 0$. As we stated in section II, ϕ_b and the corresponding ξ_E represent the characteristic concentration and correlation length in the problem, chosen for convenience to scale all concentrations and lengths.

The surface tension in this case can be written as

$$\gamma_{in} - \gamma_0 = \frac{T\phi_b}{6a\xi_E}\left[-\tilde{\kappa}\theta^2(\tilde{b}) + \int_0^{\tilde{b}}[(\theta^2-1)^2 + (\tilde{\nabla}\theta)^2]\left(\frac{\tilde{r}}{\tilde{b}}\right)^2 d\tilde{r}\right] \quad \text{(III.18)}$$

In Figure 4 we plot a polymer concentration profile. ϕ_b and ξ_E are both functions of the radius. Qualitatively, as the size of the sphere shrinks, the average concentration becomes larger, so ϕ_b increases and the correlation length ξ_E becomes shorter. Asymptotically, when the radius of the sphere becomes so small that the interaction between monomers completely dominates the attraction of the wall, then $\phi_b \sim b^{-3}$ and $\xi_E \sim b^{3/2}$ from the definition of ξ_E.

Figure 5 shows the surface tension as a function of the radius of the sphere. The minimum in surface tension indicates a balance between surface attraction and monomer–monomer repulsion. As predicted from the perturbation calculation, the surface tension starts to decrease when the surface is bent toward the solution. If we continue to reduce the size of the sphere, eventually the average concentration of monomers increases to the point where the excluded volume repulsion dominates, and the surface tension begins to increase at some critical radius. This critical radius depends on the relative strength of the attraction of the wall and the excluded volume repulsion; the stronger the attraction of the wall, the smaller the critical radius will be.

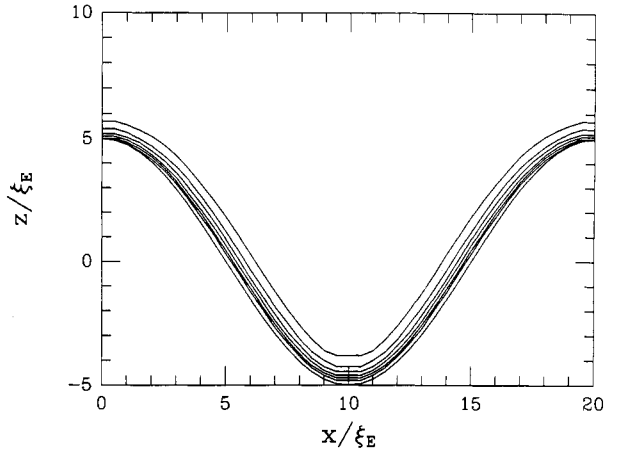

Figure 6. Contour plot of the concentration profile for $\tilde{\kappa} = 1$, $\tilde{z}_0 = 5$, and $\tilde{\lambda} = 20$. The uppermost line corresponds to $\theta = 1.1$; the separation between each line is $\Delta\theta = 0.1$.

IV. Adsorption on a Sinusoidal Grating

We now consider a polymer solution in contact with a cylindrical sinusoidal surface: $z = z_0 \cos((2\pi/\lambda)x)$. There are four fundamental lengths in the problem: surface amplitude z_0, wavelength λ, correlation length ξ_E, and κ^{-1}, which characterizes the strength of attraction of the wall. As before, it is convenient to refer all lengths to ξ_E, leaving as the relevant dimensionless length parameters $\tilde{z}_0 = z_0/\xi_E$, $\tilde{\lambda} = \lambda/\xi_E$, and $\tilde{\kappa} = \kappa/\xi_E$. The fundamental equations that determine the concentration profile θ are eq II.11 and II.12. Numerical solution of these gives the monomer distribution. We consider various limiting regimes for the three dimensionless length parameters.

1. $\tilde{\lambda} \gg 1$. Here we expect only perturbative changes from the flat-surface results, since the wavelength of the surface fluctuation is much larger than the correlation length. Then the polymer solution can be influenced only by the local curvature of the surface; this is borne out by the numerical results (Figure 6). The calculation shows that the density of monomers on the surface is a maximum at the valley and a minimum at the peak, as predicted from the perturbational results of section III; these conclusions hold for both strong and weak adsorption.

2. $\tilde{\lambda} \lesssim 1$, $\tilde{z}_0 > 1$. Figure 7 shows the monomer distribution when $\tilde{\lambda} \sim 1$ and $\tilde{z}_0 \sim 1$. The density of monomers increases toward the bottom of the valley, where it is higher than the density at a flat surface with the same attractive strength. As the surface oscillation amplitude $\tilde{z}_0$ grows much larger than the correlation length, this tendency for polymer condensation in the vicinity of the valley becomes more obvious (Figure 8). We can gain some analytic understanding of this tendency by recognizing that when $z_0 \gg \lambda, \xi_E$, the polymer density distribution between two adjacent peaks (excluding the regions near the extremes), should be approximately the same as it is between two infinite parallel plates of the same material in the polymer solution. de Gennes[13] has investigated the force between two such plates using a mean field approach. Here we study the density of monomers asymptotically as the gap between the plates becomes very narrow.

We denote by $\phi(x)$ the volume fraction of polymers, where x is the direction perpendicular to the plates. The origin is chosen to be the midpoint of the gap, which is of

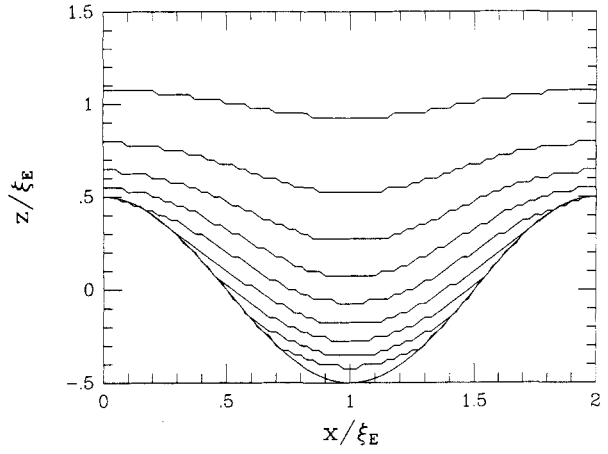

Figure 7. Contour plot of the concentration profile for $\tilde{\kappa} = 1$, $\tilde{z}_0 = 0.5$, and $\tilde{\lambda} = 2$. The uppermost line corresponds to $\theta = 1.1$; the separation between each line is $\Delta\theta = 0.1$.

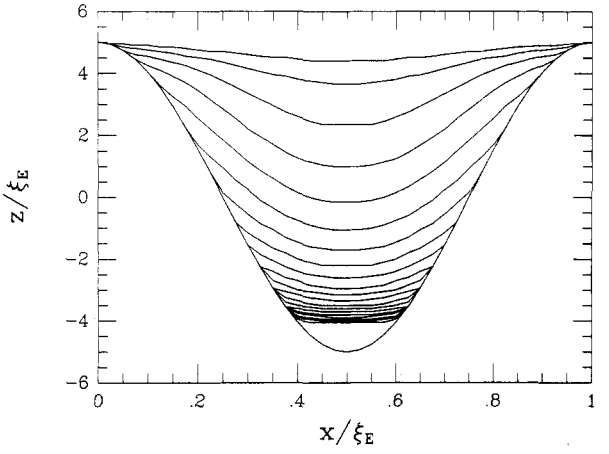

Figure 8. Contour plot of the concentration profile for $\tilde{\kappa} = 1$, $\tilde{z}_0 = 5$, and $\tilde{\lambda} = 1$. The uppermost line corresponds to $\theta = 1.4$; the separation between each line is $\Delta\theta = 0.1$.

width $2h$. As before, we define $\theta^2 \equiv \phi/\phi_b$; then θ satisfies the equations

$$\frac{d^2\theta}{d\tilde{x}^2} = 2\theta(\theta^2 - 1) \qquad \text{(IV.1)}$$

$$\frac{1}{\theta}\frac{d\theta}{d\tilde{x}}\bigg|_{\tilde{x}=\tilde{h}} = \tilde{\kappa} \qquad \text{(IV.2)}$$

The first integral of eq IV.1 gives

$$\left(\frac{d\theta}{d\tilde{x}}\right)^2 = (\theta^2 - 1)^2 + C \qquad \text{(IV.3)}$$

The condition at $\tilde{x} = 0$ is, by symmetry, $d\theta/d\tilde{x} = 0$. If θ_m and θ_s are values of θ at the midpoint and at the surface respectively, then $C = -(\theta_m^2 - 1)^2$, and we have from eq IV.3

$$\tilde{h} = \int_{\theta_m}^{\theta_s} \frac{d\theta}{[(\theta^2 - 1)^2 - (\theta_m^2 - 1)^2]^{1/2}} \qquad \text{(IV.4)}$$

and the boundary condition (IV.2) becomes

$$\frac{[(\theta_s^2 - 1)^2 - (\theta_m^2 - 1)^2]^{1/2}}{\theta_s} = \tilde{\kappa} \qquad \text{(IV.5)}$$

From eq IV.4 and IV.5 we can determine θ_m and θ_s. In the narrow-gap limit $\tilde{h} \ll 1$, we can solve for θ_m and θ_s self-consistently; assuming both to be large compared to unity, we find

$$\theta_m \sim \theta_s \approx \left(\frac{\tilde{\kappa}}{2\tilde{h}}\right)^{1/2} \qquad (\tilde{h} \ll 1) \qquad \text{(IV.6)}$$

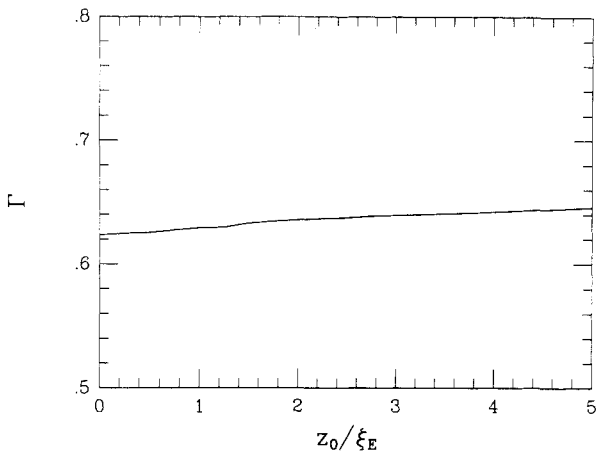

Figure 9. Surface excess as a function of surface roughness amplitude, $\tilde{z}_0$. Here $\tilde{\kappa} = 1$ and $\tilde{\lambda} = 2$.

Thus the average density of polymer between the plates increases as the gap narrows:

$$\langle\phi\rangle \approx \frac{\tilde{\kappa}}{2\tilde{h}}\phi_b \qquad (\tilde{h} \ll 1) \qquad \text{(IV.7)}$$

or

$$\langle\phi\rangle \approx \frac{\kappa a^2}{3\upsilon h} \qquad \text{(IV.8)}$$

That is, within mean-field theory, the total number of monomers between the plates becomes independent of gap width h at small h. Furthermore, this number is a function only of κ and υ, independent of the bulk concentration ϕ_b.

Surface Excess. The surface excess calculated here is defined as

$$\Gamma a^3 = \frac{1}{L}\int dl \int_{z(x)}^{\infty} dz\ (\phi - \phi_b) \qquad \text{(IV.9)}$$

where l is measured along the surface, $z(x)$ is the height of the surface, and the integral is taken over a single period (length λ) in x.

In Figure 9 we plot surface excess against surface roughness amplitude $\tilde{z}_0$. We can see that the surface excess increases slowly with $\tilde{z}_0$ from its flat surface value.

V. Discussion

When a semidilute polymer solution is put in contact with an adsorbing wall, it forms an adsorption layer near the wall, the characteristic thickness of which is the correlation length ξ_E. The strength of the wall attraction only affects the detailed concentration profile within the layer; it does not change the layer thickness. The surface free energy consists of two parts:

$$U - U_0 = -\gamma_1\int dS\ \phi + (T/a^3)\int dV\left[\frac{1}{2}\upsilon\phi^2 + \frac{a^2}{24\phi}(\nabla\phi)^2\right] \qquad \text{(V.1)}$$

The first term represents the surface attraction, proportional to the surface area. The second term is the contribution of the interaction betweem monomers and of the entropy associated with the deviation from uniform density; both grow with the volume over which $\phi - \phi_b$ is appreciable and thus are roughly proportional to the volume of the adsorption layer. Qualitatively, when a flat surface is deformed into a sphere, with the polymer solution outside it, the adsorption layer formed has a larger volume per unit surface area, so the surface energy is higher than

it was for the flat surface, and the surface tension therefore increases. It should be pointed out that apart from the change in the layer volume, there is another countervailing effect: the surface concentration and the average concentration in the layer are both reduced in this case, making both parts of the free energy smaller, but that seems to be quantitatively less important, so that the layer volume change is the dominant feature. Correspondingly, if the polymer is inside the sphere, the volume of the adsorption layer per unit surface area is reduced, and the surface tension is lower than it was for the flat surface. But since the volume interaction term is proportional to ϕ^2, whereas the surface interaction is proportional to ϕ, if the size of the sphere is reduced sufficiently, ϕ becomes large enough that the volume term dominates, and the surface tension will start to increase with further reduction in sphere radius.

For polymer adsorption on a sinusoidal surface, when $\lambda \gg \xi_E$ or $z_0 \ll \xi_E$, i.e., the surface variation is either slow or small, the problem is perturbational, as shown in the contour plot of polymer density distribution. The interesting case is when we have rapid and large amplitude surface fluctuation, i.e., when $\lambda \ll \xi_E$ and $z_0 \gg \xi_E$. The calculation shows that it is favorable for the polymer to fill the deep holes or valleys on a rough surface, although kinetically it may take a long time for polymers to arrive at this equilibrium distribution. In section IV we used two parallel plates as a model of the steep sided sinusoidal surface and studied the behavior of the density between the plates as this separation decreased. Here we study the parallel plate problem in terms of the appropriate free energy functional, which allows us to go beyond mean-field theory to a scaling approach.

In the mean-field approximation

$$\gamma - \gamma_0 \sim -\tilde{\kappa}\theta_s^2 + \int d\tilde{x}\, [(\theta^2 - 1)^2 + (\tilde{\nabla}\theta)^2] \quad \text{(V.2)}$$

When $h \ll \xi_E$, $\theta_s \sim \theta_m \gg 1$, and then

$$\gamma - \gamma_0 \sim -\tilde{\kappa}\langle\theta\rangle^2 + \tilde{h}\langle\theta\rangle^4 \quad \text{(V.3)}$$

Minimization of γ then gives

$$\langle\theta\rangle^2 \sim \tilde{\kappa}/\tilde{h} \quad \text{(V.4)}$$

The scaling free energy functional takes the form

$$\gamma - \gamma_0 \sim -\gamma_1\phi_s + T\int dx \left[\xi^{-3}(\phi) + \frac{1}{\xi(\phi)}\left(\frac{d\phi}{dx}\right)^2\right] \quad \text{(V.5)}$$

where $\xi(\phi)$ is the local correlation length, defined as $\xi(\phi) = a\phi^{-3/4}$. If we minimize this free energy, we find

$$\langle\phi\rangle \sim (\kappa/h)^{4/5} \quad \text{(V.6)}$$

As compared with the mean field result $\langle\phi\rangle \sim \kappa/h$, the density increases more slowly. This is due to the fact that the actual monomer–monomer interaction grows more rapidly with polymer density that is suggested by the mean-field approximation. This expels more monomers from the gap as it is narrowed. The total number of monomers in the gap in this case will go to zero asymptotically as $N \sim h^{1/5}$.

Acknowledgment. We thank Dr. Guiseppe Rossi and Prof. P. A. Pincus for many helpful discussions. This work was supported in part by the Department of Energy through Grant No. DE-FG03-87ER45288 and in part by the National Science Foundation under Grant No. PHY 8217853, supplemented by funds from the National Aeronautics and Space Administration.

References and Notes

(1) de Gennes, P.-G. *Rep. Prog. Phys.* **1969**, *32*, 187.
(2) de Gennes, P.-G. *Macromolecules* **1981**, *14*, 1637.
(3) Jones, I. S.; Richmond, P. *J. Chem. Soc., Faraday Trans. II* **1977**, *73*, 1062.
(4) Ober, R.; Paz, L.; Taupin, C.; Pincus, P.; Boileau, S. *Macromolecules* **1983**, *16*, 50.
(5) di Meglio, J. M.; Ober, R.; Paz, L.; Taupin, C.; Pincus, P.; Boileau, S. *J. Phys. (Les Ulis, Fr.)* **1983**, *44*, 1035.
(6) Fleer, G. J.; Scheutjens, J. M. H. M. *Adv. Colloid Interface Sci.* **1982**, *16*, 341.
(7) Eisenriegler, E.; Kremer, K.; Binder, K. *J. Chem. Phys.* **1982**, *77*, 6296.
(8) de Gennes, P.-G.; Pincus, P. *J. Phys. (Les Ulis, Fr.)* **1983**, *44*, L-241.
(9) Pincus, P. A.; Sandroff, C. J.; Witten, T. A. *J. Phys. (Les Ulis, Fr.)* **1984**, *45*, 725.
(10) Hone, D.; Ji, H.; Pincus, P. *Macromolecules* **1987**, *20*, 2543.
(11) Cahn, J. W.; Hilliard, J. E. *J. Chem. Phys.* **1957**, *28*, 1958.
(12) de Gennes, P.-G. *Scaling Concepts in Polymer Physics*; Cornell University: Ithaca, NY, 1979.
(13) de Gennes, P.-G. *Macromolecules* **1982**, *15*, 492.
(14) Edwards, S. *Proc. Phys. Soc., London* **1965**, *85*, 613.